CrystEngComm

Development of Protein Seed Crystals Reinforced by High-Strength Hydrogels

Journal:	*CrystEngComm*
Manuscript ID:	CE-ART-04-2015-000844.R1
Article Type:	Paper
Date Submitted by the Author:	24-May-2015

Complete List of Authors:	Sugiyama, Shigeru; Osaka University, Graduate School of Engineering; Shimizu, Noriko; Osaka University, Graduate School of Engineering Kakinouchi, Keisuke; SOSHO Inc., Hiraoka, Osamu; Shujitsu University, School of Pharmacy Matsumura, Hiroyoshi; Osaka University, Graduate School of Engineering Yoshikawa, Hiroshi; Saitama University, Department of Chemistry Takahashi, Yoshinori; Osaka University, Graduate School of Engineering Maruyama, Mihoko; Osaka University, Graduate School of Engineering Yoshimura, Masashi; Osaka University, Graduate School of Engineering Adachi, Hiroaki; SOSHO Inc., Takano, Kazufumi; Kyoto Prefectural University, Graduate School of Life and Environmental Sciences Murakami, Satoshi; Tokyo Institute of Technology, Graduate School of Bioscience and Biotechnology Inoue, Tsuyoshi; Osaka University, Graduate School of Engineering Murata, Michio; Osaka University, Graduate School of Science Mori, Yusuke ; Osaka University, Graduate School of Engineering

Development of Protein Seed Crystals Reinforced by High-Strength Hydrogels

Shigeru Sugiyama,[1,2,*] Noriko Shimizu,[3] Keisuke Kakinouchi,[4] Osamu Hiraoka,[5] Hiroyoshi Matsumura,[3,4,#] Hiroshi Y. Yoshikawa,[6] Yoshinori Takahashi,[3] Mihoko Maruyama,[3] Masashi Yoshimura,[3] Hiroaki Adachi,[4] Kazufumi Takano,[4,7] Satoshi Murakami,[4,8] Tsuyoshi Inoue,[3,4] Michio Murata,[1,2] and Yusuke Mori[3,4]

[1] Graduate School of Science, Osaka University, Toyonaka, Osaka 560-0043 Japan

[2] JST, ERATO, Toyonaka, Osaka 560-0043 Japan

[3] Graduate School of Engineering, Osaka University, Suita, Osaka 565-0871 Japan

[4] SOSHO Inc., 2-1 Yamadaoka, Suita, Osaka 565-0871 Japan

[5] School of Pharmacy, Shujitsu University, Okayama 703-8516 Japan

[6] Department of Chemistry, Saitama University, Saitama 338-8570 Japan

[7] Graduate School of Life and Environmental Sciences, Kyoto Prefectural University, Kyoto 606-8522 Japan

[8] Graduate School of Bioscience and Biotechnology, Tokyo Institute of Technology, Nagatsuta, Midori-ku, Yokohama 226-8501 Japan

Abstract

Neutron macromolecule crystallography can determine the positions of hydrogen atoms in proteins, thereby clarifying the protein structure and function as well as enzyme mechanisms. It requires very large crystals to make up for the low flux of available neutron beams. Some techniques have been developed to obtain large protein crystals. However, problems remain with the handling of the crystal. Here we propose a novel crystallization technique that combines high-strength hydrogel and seeding methods with fatty-acid binding protein and lysozyme. This novel approach enables safe introduction of seeds into pre-equilibrated protein solutions without damage. Consequently, we can grow large single crystals without forming twinned crystals and polycrystals. This technique is expected to expand the scope of important proteins and may lead to an automated system for high-resolution X-ray and neutron crystallography.

Introduction

X-ray macromolecule crystallography is a powerful tool for determining the three-dimensional (3D) structure of proteins with atomic resolution. The 3D structures of proteins provide useful information on not only the structure-function relationship, but also the structure-based drug design. However, X-ray crystallographers rarely use hydrogen atoms and hydration water molecules to gain a more detail understanding of the protein structure.[1] Neutron macromolecule crystallography provides insight into protein structure protonation details.[2] This technique yields better understanding of the enzyme mechanism and promotes rational structure-based drug design. One important purpose of neutron macromolecule crystallography is to obtain extremely large protein crystals (e.g., 1 to 6 mm^3)[1] to compensate for the weak flux of the available neutron beam.[3, 4] To date, techniques for obtaining large protein crystals include macroseeding,[5] the slow-cooling method,[6] the floating-and-stirring technique,[7] the large-scale hanging drop method,[8] and top-seeded solution growth.[9, 10] However, several obstacles remain with these methods. For example, with the macroseeding technique that is frequently utilized to enlarge protein crystals, we must pay scrupulous attention when handling the seed crystal. A seed crystal is introduced into a pre-equilibrated protein solution, and this cycle is repeated several times. However, it is often difficult to use a seed crystal because protein crystals are usually very small and fragile.[11]

To overcome the disadvantage of very small and fragile seed crystals, we used high-strength agarose and thermoreversible gelation synthetic polymer (TGP)[12] hydrogels. Agarose and TGP are used in protein crystallization to control nucleation of the protein crystals.[13-16] They reduce convection and prevent crystal sedimentation,[17] resulting in high-quality protein crystals.[18] We recently developed a new method for growing protein crystals in high-strength hydrogels.[19-26] Our recent study demonstrated that these high-strength hydrogels increase the crystal's mechanical stability while considerably reducing osmotic shock,[27] in part because incorporating hydrogel fibers into the crystal during growth significantly strengthens the crystal.

Here we propose the novel combinational technique of seeding and reinforcing hydrogel-grown

protein crystals using agarose or TGP hydrogels for neutron crystallography. To evaluate the feasibility and efficacy of this new approach, we optimized this technique for human heart-type fatty-acid binding protein (FABP3) and chicken egg-white lysozyme (LZM) using agarose or TGP hydrogels. Furthermore, we grew larger high-quality crystals of FABP3 and LZM using repeat seeding. These crystals were used for X-ray diffraction (XRD) measurements, followed by structural analysis. No obvious differences were observed in the crystal data between the hydrogel-grown seed and seed-grown crystals. The resulting electron densities were also clear for the entire polypeptide consisting of these model proteins. We believe that this new approach expands the scope of target proteins and may lead to an automated system for X-ray and neutron crystallographic analysis.

Experimental

Protein and hydrogel preparations

The human heart-type fatty acid-binding protein (hFABP3) was expressed and purified according to the previously described protocol.[28, 29] Purity was verified using sodium dodecyl sulfate polyacrylamide electrophoresis. Chicken egg-white lysozyme (LZM) was purchased from Seikagaku Kogyo and used without further purification.

Sea plaque agarose hydrogel (agaroseSP)[30] and TGP known as Mebiol gel were prepared according to the previously described protocol.[16, 26] AgaroseSP was purchased from Takara Bio. The gelling temperature of the agaroseSP is 299 to 303K. Here, 4.5% (w/v) agaroseSP solution was prepared by slowly stirring agarose powder in water at room temperature (295K) and melted at 373K. Before setting up the crystallization trials, the agaroseSP was remelted at 368K and maintained as liquid at 308K. TGP was purchased from Mebiol, Inc. (Kanagawa, Japan, through Ikeda Scientific Co., Ltd., Tokyo, Japan).[31-34] TGP is a copolymer composed of thermoresponsive polymer blocks and hydrophilic polymer blocks.[35] This polymer block is hydrophilic at temperatures below 293K and hydrophobic at temperatures above 293K, forming cross-linking points and a homogenous 3D network of Mebiol. The gelling temperature of TGP is 293K. TGP was dissolved in distilled water at 277K for 3 days. The 15% (w/v) TGP sol solution was prepared and then stored at 277K.

Crystallization and seeding

Seed crystals of the proteins were prepared using the batch method. In addition, large crystals were grown by combining high-strength hydrogel and seeding. Purified FABP3 samples in buffer (20mM Tris-HCl, 100mM NaCl, pH 8.0) were concentrated to 60mg/ml for crystallization. LZM was dissolved in 0.1M sodium acetate buffer at pH 4.5 to protein concentrations of 60mg/ml. These protein solutions were passed through a 0.22 μm pore filter (Advantec DISMIC-25). The crystallization solutions for seed crystals were prepared by mixing equal volumes (1.5μl) of protein solution (FABP3, 60mg/ml; LZM, 60mg/ml), precipitating agent (FABP3, 60% PEG400; LZM, 9.0%

NaCl), and hydrogel (FABP3, 4.5% agarose; LZM, 4.5% agarose or 15% TGP) at 310K for agarose or 277K for TGP. The final agaroseSP (TGP) concentration was 1.5% (5.0%). AgaroseSP (1.5 to 2.0%) is able to maintain the sol state at 310K for 16 hours and gelates rapidly at less than 293K. Therefore, the mixed drop solutions (4.5μl) were immediately loaded onto CombiClover plates (Emerald BioSystems) during the sol state, and the plates were covered with 0.055mm-thick sealing tape (NITTO DENKO CORPORATION). The crystallization conditions for obtaining large protein crystals were the same as those for seed crystals except protein concentrations. The seed crystals were carefully removed using Microknife and Crystal Remover tools (SOSHO, Inc., Osaka, Japan). The processed hydrogels containing seed crystals could then be captured using a cryoloop with little damage to the crystals, and they were introduced into the crystallization solutions without hydrogels to obtain large protein crystals. Table 1 summarizes the crystallization and seeding conditions of the proteins used in this study.

Data Collection and structure determination

XRD experiments were performed under cryogenic conditions. The hydrogel-grown seed crystals were carefully removed using Microknife as described above. A thickness of the gel surrounding the seed crystals was approximately 0.2 mm after the processing operation. Next, the seed-grown crystals were soaked in cryoprotectant solution (FABP3, 55% PEG400; LZM, 30% glycerol) and then directly flash-cooled in a stream of cold nitrogen gas at 100K on the goniometer head of the XRD equipment. XRD data were collected using beamlines from the SPring-8 synchrotron radiation sources (Harima, Japan) and a Rigaku R-AXIS V imaging plate using CuKα radiation produced with a Rigaku ultra X18 rotating anode generator. These data were processed and scaled using HKL-2000.[36] The deposited FABP3 (PDB ID 3WVM)[28] and LZM (PDB ID 193L)[37] structure coordinates were used as starting models for structural analysis of FABP3 and LZM. The model was manually improved using COOT.[38] Structural refinements were carried out using a restrained least-squares refinement method in Refmac software[39] as implemented within the CCP4 package.

The geometry of the refined model was validated using PROCHECK.[40] The data collection and refinement statistics are summarized in Table 2. Representative portions of the $(2|F_o|-|F_c|)$ electron-density map after refinement are depicted in Figure 4.

Results and discussion

Combination of high-strength hydrogel and seeding methods

Here, we briefly describe some practical advantages of crystals grown in high-strength hydrogels. Hydrogel-grown crystal trapped in hydrogel fibers exhibits increased tolerance to environmental perturbations (e.g., evaporation and temperature change), as well as vibration generated during transportation.[26, 41, 42] Hydrogel-grown crystals may thus overcome significant problems (e.g., evaporation, temperature change, and vibration) caused by introducing a seed crystal into a pre-equilibrated protein solution. We could handle hydrogel-grown crystals without touching them directly by easily capturing them from the solution using a cryoloop.[16, 19] The hydrogel surrounding the crystals protected them while serving as an anchor to fix them on the cryoloop, significantly reducing physical damage to the crystals. Furthermore, crystal sedimentation was prevented, and the crystals were immobilized in a crystallization drop,[20, 21] enabling us to suppress the production of polycrystal at the initial step of crystal growth and to select the best single crystal for the seeding experiment under direct microscopic observation (Figure 1). With this method, the agarose-grown seed crystal of FABP3 grew to $0.5 \times 0.2 \times 0.2$mm ($0.020$mm^3), the agarose-grown seed crystal of LMZ grew to $0.5 \times 0.1 \times 0.1$mm ($0.005$mm^3), and the TGP-grown seed crystal of LZM grew to $0.3 \times 0.3 \times 0.3$ mm (0.027 mm^3).

Crystals are usually produced in highly supersaturated solutions where spontaneous nucleation of the crystals usually occurs. However, nuclei spontaneously generated in these solutions grow rapidly after nucleation, leading to poor crystallinity and the formation of many polycrystals. Thus, these crystals may be unsuitable for diffraction studies. In such cases, each condition must be optimized separately. The seeding method, which introduces a seed crystal into an appropriately saturated solution, is generally used to solve this problem. However, protein crystals are usually very small and fragile. If the seed crystals become firmly attached to a crystal growth vessel, it is difficult to remove them without significant damage. To solve this problem, we combined high-strength hydrogel and seeding methods. Figure 1a illustrates the protocol for transporting the seed crystal

using this combination of methods.

Optimization of crystallization conditions

We previously reported that the nucleation of proteins is significantly promoted by highly concentrated hydrogels, solving serious repeatability problems caused by the low nucleation rate in protein crystallization.[16, 23] One feasible explanation for this phenomenon is that highly concentrated hydrogels may trap more water molecules in the crystallization solution, and thereby decrease protein solubility and promoted nucleation, resulting in high-quality crystals. However, conditions for producing large high-quality crystals are often affected by the crystallization setup. Therefore, we optimized the crystallization conditions of FABP3 and LZM by combining high-strength hydrogel and seeding methods. First, hydrogel-grown seed crystals of FABP3 and LZM were obtained in 1.5% agarose or 5.0% TGP hydrogels at protein concentrations of 20mg/ml using the batch method. The hydrogel concentrations were optimized at somewhat lower concentrations than usual (2.0% agarose, 6.0% TGP) to control nucleation of protein crystals. Next, these seed crystals were introduced into the same conditions without hydrogels. However, as depicted in Figure 2, the protein concentration triggered nucleation of small crystals within one week. For FABP3, polycrystallization of the seed crystal also occurred at protein concentrations of 6 or 9mg/ml, although the seed crystals themselves also grew. These results suggest that no seed crystals grow as large high-quality crystals under these conditions. Finally, hydrogel-grown FABP3 and LZM seed crystals were grown under the same conditions but with protein concentrations of 3mg/ml for the FABP3 seed crystals and 10mg/ml for the LZM crystals (Table 1). The seed crystals grew larger, and no additional nucleation was generated under these optimized conditions (Figures 1a, b, and c). Hydrogel-grown LZM seed crystals were observed at the center of the seed-grown crystals. These results demonstrate that crystals grew on only the hydrogel-grown seed crystals introduced into the crystallization solution. As a result, an seed-grown crystal of FABP3 grew to $1.3 \times 1.0 \times 1.0$mm ($1.3$mm^3), and two seed-grown crystals (agarose and TGP) of LZM each grew to $1.2 \times 1.0 \times 1.0$mm ($1.2$mm^3).

X-ray diffraction studies

To examine the diffraction quality of seed-grown FABP3 and LZM crystals, XRD experiments were performed under cryogenic conditions using seed-grown crystals soaked in crystallization solution containing 55% (w/v) PEG400 or 30% (w/v) glycerol. For XRD measurements at SPring-8, to evaluate the quality of the crystal growth layer that developed on the hydrogel-grown seed crystal, a seed-grown LZM crystal was exposed to 50μm X-ray beams focused on the layer that grew on an agarose hydrogel-grown LZM seed crystal. In addition, other seed-grown crystals were exposed to X-ray beams focused on the center of these crystals. The diffraction pattern exhibited sharp and clear diffraction spots without splits or blurs (Figure 3), suggesting high crystallinity of the seed-grown FABP3 and LZM crystals without forming twinned crystals and polycrystals. This result indicates that seed-grown crystals conserve the same growth direction as seed crystals. The diffraction quality of the seed-grown FABP3 and LZM crystals was satisfactory for 3D structure determination. These experiment results suggest that hydrogel-grown seed crystals can be safely introduced into pre-equilibrated protein solutions without suffering damage.

Next, these diffraction data were processed and scaled to compare the XRD data statistics of hydrogel-grown and seed-grown crystals. This comparison indicated no significant differences in unit-cell dimensions and estimated mosaicity (Table 2), although XRD data of agarose-grown and seed-grown LZM crystals were collected using different X-ray sources and wavelengths. These results confirm that the excess of hydrogels surrounding FABP3 and LZM seed crystals does not significantly affect the XRD quality of crystals.

Crystal structure analyses and structural comparison

X-ray structural analyses were carried out to clarify differences in the structures of hydrogel-grown and seed-grown crystals (Figure 4). The resulting electron densities were clear for the entire polypeptide of FABP3 and LZM, thus demonstrating the high quality of the structural

analysis. We compared the structures of hydrogel-grown crystals with the 3D structures determined from the seed-grown FABP3 and LZM crystals. The root-mean-square deviations (RMSDs) were evaluated to be 0.06Å for 460 main-chain atoms between the agaroseSP-grown and seed-grown FABP3 crystal structures. The RMSDs were an average of 0.20Å for 516 main-chain atoms between structures of the agaroseSP-grown and seed-grown LZM crystals with agaroseSP, and an average of 0.25Å between structures of the TGP-grown and seed-grown LZM crystals with TGP. These results clearly demonstrate that the structures of the seed-grown crystals were almost the same as those of the hydrogel-grown crystals.

Advantages of the combinational technique

The novel combination of hydrogel and seeding methods for obtaining larger crystals has the following advantages. First, hydrogel-grown seed crystals are protected by the high-strength hydrogel surrounding the crystals, enabling direct contactless manipulation of very fragile crystals. This technique is quite effective in repeated macroseeding experiments, since mechanical damage to the protein crystals caused by direct contact generates nucleation and polycrystallization. Second, in seeding experiments, the crystals are exposed to evaporation during manipulation (e.g., separating a single crystal from a polycrystal, removing the crystal from the growth vessel, and transporting the crystal to a new crystallization solution) under microscopic observation, because such treatment provokes evaporation of the crystallization drop solution containing the crystals. As a result, long-term exposure to evaporation seriously damages the seed crystals, resulting in drying out and cracking. It is very difficult to carry out these operations without damaging the crystals. However, as previously reported,[25] hydrogel-grown crystals have a high tolerance for environmental perturbations under evaporation conditions, enabling us to manipulate seed crystals without significant damage. Third, this method can be applied to manipulating microcrystals for seeding experiments by removing the microcrystal with hydrogels, with the protein sample that can obtain only microcrystals. Fourth, since this method reduces crystal sedimentation and fixes the crystal in a crystallization drop,

we can easily manipulate the best single crystal under direct microscopic observation. These advantages suggest that this technique is useful for automating microcrystal and macrocrystal seeding operations.

Conclusion

Large crystals of FABP3 and LZM were successfully obtained by combining high-strength hydrogel and seeding techniques, demonstrating that this method may be applied for general use. In this study, we found that the crystal layer that developed on hydrogel-grown seed crystals has the following characteristics. In macroseeding, spontaneous nucleation frequently occurs during crystal growth, causing polycrystallization of seed crystals. The diffraction spots of a seed-grown crystal using this technique made the crystal suitable for 3D structure determination without splitting or blurring, indicating a single crystal. Also, comparison of the diffraction data statistics of seed crystal and those of seed-grown crystal exhibited no distinct differences. Thus, the use of the hydrogel-grown crystals as seed crystals enables us to grow large high-quality single crystals without causing damage. This novel combinational technique poses the possibility of developing a fully automated system for generating large single protein crystals.

Associated Content

Author Information

Corresponding Author

*E-mail: sugiyama@cryst.eei.eng.osaka-u.ac.jp.

Telephone: +81-66879-7701.

Present Addresses

College of Life Sciences, Ritsumeikan University, Kusatsu, Shiga 525-8577 Japan

Notes

The authors declare no competing financial interest.

Acknowledgement

We thank E. Yamashita and A. Nakagawa on BL44XU and K. Baba and N. Mizuno on BL38B1 for the data collection at SPring-8 (Hyogo, Japan). The synchrotron radiation experiments were performed at SPring-8 with the approval of the Japan Synchrotron Radiation Research Institute (JASRI) (Proposal nos. 2013A/B6827, 2014A/B6928, and 2014B1195). This work was supported in part by JSPS KAKENHI (Japan) Grants 23860028 (S.S.), 25650051 (S.S.), 25286051 (S.S.), Astellas Foundation for Research on Metabolic Disorders, and Platform for Drug Discovery, Informatics, and Structural Life Science from the Ministry of Education, Culture, Sports, Science and Technology, Japan.

References

(1) D. A. A. Myles, F. Dauvergne, M. P. Blakeley, F. Meilleur, *J. Appl. Cryst.*, 2012, **45**, 686–692.
(2) N. Niimura, *Curr. Opin. Struct. Biol.*, 1999, **9**, 602–608.
(3) M. Maeda, T. Chatake, I. Tanaka, A. Ostermann, N. Niimura, *J Synchrotron Radiat*., 2004, **11**, 41–44.
(4) S. Arai, T. Chatake, Y. Minezaki, N. Niimura, *Acta Crystallogr.*, 2002, **D58**, 151–153.
(5) S. L. Mowbray in "Protein Crystallization" pp 155. Eds: T.M. Bergfors, International University Line, La Jolla, CA., 1999.
(6) H. Matsumura, M. Adachi, S. Sugiyama, S. Okada, M. Yamakami, T. Tamada, K. Hidaka, Y. Hayashi, T. Kimura, Y. Kiso, T. Kitatani, S. Maki, H.Y. Yoshikawa, H. Adachi, K. Takano, S. Murakami, T. Inoue, R. Kuroki, Y. Mori, *Acta Crystallogr.*, 2008, **F64**, 1003–1006.
(7) N. Shimizu, S. Sugiyama, M. Maruyama, Y. Takahashi, M. Adachi, T. Tamada, K. Hidaka, K. Kimura, Y. Kiso, H. Adachi, K. Takano, S. Murakami, T. Inoue, R. Kuroki, Y. Mori, H. Matsumura, *Cryst. Growth Des.*, 2010, **10**, 2990–2994.
(8) K. Kakinouchi, T. Nakamura, T. Tamada, H. Adachi, S. Sugiyama, M. Maruyama, Y. Takahashi, K. Takano, S. Murakami, T. Inoue, R. Kuroki, Y. Mori, H. Matsumura, *J. Appl. Crystallogr.*, 2010, **43**, 937–939.
(9) N. Shimizu, S. Sugiyama, M. Maruyama, H. Y. Yoshikawa, Y. Takahashi, M. Adachi, K. Takano, S. Murakami, T. Inoue, H. Matsumura, Y. Mori, *Cryst. Growth Des*., 2009, **9**, 5227–5232.
(10) M. Adachi, T. Ohhara, K. Kurihara, T. Tamada, E. Honjo, N. Okazaki, S. Arai, Y. Shoyama, K. Kimura, H. Matsumura, S. Sugiyama, H. Adachi, K. Takano, Y. Mori, K. Hidaka, T. Kimura, Y. Hayashi, Y. Kiso, R. Kuroki, *Proc. Natl. Acad. Sci. U.S.A.*, 2009, **106**, 4641–4646.
(11) B. W. Matthews, *Annu. Rev. Phys. Chem.*, 1976, **27**, 493–523.
(12) H. N. Madhavan, J. Malathi, R. P. Joseph, Y. Mori, S. J. K. Abraham, H. Yoshioka, Curr. Sci., 2004, **87**, 1275−1277.
(13) O. Vidal, M. C. Robert, F. Boué, *J. Crystal Growth*, 1998, **192**, 257–270.
(14) C. Biertumpfel, J. Basquin, D. Suck, C. Sauter, *Acta Crystallogr.,* 2002, **D58**, 1657–1659.
(15) J. M. García-Ruiz, *Methods Enzymol.,* 2003, **368**, 130–154.
(16) S. Sugiyama, N. Shimizu, G. Sazaki, M. Hirose, Y. Takahashi, M. Maruyama, H. Matsumura, H. Adachi, K. Takano, S. Murakami, T. Inoue, Y. Mori, *Cryst. Growth Des.*, 2013, **13**, 1899–1904.
(17) M. C. Robert, F. Lefaucheux, B. Jannot, G. Godefroy, E. Garnier, *J. Crystal Growth,* 1988, **88**, 499–510.
(18) D. W. Zhu, B. Lorber, C. Sauter, J. D. Ng, P. Benas, C. L. Grimellec, R. Giege, *Acta Crystallogr.,* 2001, **D57**, 552–558.
(19) S. Sugiyama, K. Tanabe, M. Hirose, T. Kitatani, H. Hasenaka, Y. Takahashi, H. Adachi, K. Takano, S. Murakami, Y. Mori, T. Inoue, H. Matsumura, *Jpn. J. Appl. Phys.,* 2009, **48**, No.075502.
(20) S. Sugiyama, H. Hasenaka, M. Hirose, N. Shimizu, T. Kitatani, Y. Takahashi, H. Adachi, K. Takano, S. Murakami, T. Inoue, Y. Mori, H. Matsumura, *Jpn. J. Appl. Phys.,* 2009, **48**, No.105502.
(21) H. Hasenaka, S. Sugiyama, M. Hirose, N. Shimizu, T. Kitatani, Y. Takahashi, H. Adachi, K. Takano, S. Murakami, Y. Mori, T. Inoue, H. Matsumura, *J. Cryst. Growth,* 2009, **312**, 73–78.
(22) H. Y. Yoshikawa, R. Murai, S. Sugiyama, G. Sazaki, T. Kitatani, Y. Takahashi, H. Adachi, H. Matsumura, S. Murakami, T. Inoue, K. Takano, Y. Mori, *J. Cryst. Growth,* 2009, **311**, 956–959.
(23) K. Tanabe, M. Hirose, R. Murai, S. Sugiyama, N. Shimizu, M. Maruyama, Y. Takahashi, H. Adachi, K. Takano, S. Murakami, Y. Mori, E. Mizohata, T. Inoue, H. Matsumura, *Appl. Phys. Express,* 2009, **2**, No.125501.
(24) R. Murai, H. Y. Yoshikawa, Y. Takahashi, M. Maruyama, S. Sugiyama, G. Sazaki, H. Adachi, H. Matsumura, S. Murakami, T. Inoue, K. Takano, Y. Mori, *Appl. Phys. Lett.,* 2010, **96**,

No.043702.
(25) H. Matsumura, S. Sugiyama, M. Hirose, K. Kakinouchi, M. Maruyama, H. Adachi, R. Murai, K. Takano, S. Murakami, Y. Mori, T. Inoue, *J. Synchrotron Radiat.,* 2011, **18**, 16–19.
(26) S. Sugiyama, M. Hirose, N. Shimizu, M. Niiyama, M. Maruyama, G. Sazaki, R. Murai, H. Adachi, K. Takano, S. Murakami, T. Inoue, Y. Mori, H. Matsumura, *Jpn. J. Appl. Phys.,* 2011, **50**, No.025502.
(27) S. Sugiyama, M. Maruyama, G. Sazaki, M. Hirose, H. Adachi, K. Takano, S. Murakami, T. Inoue, Y. Mori, H. Matsumura, *J. Am. Chem. Soc.,* 2012, **134**, 5786–5789.
(28) M. Hirose, S. Sugiyama, H. Ishida, M. Niiyama, D. Matsuoka, T. Hara, E. Mizohata, S. Murakami, T. Inoue, S. Matsuoka, M. Murata, *J Synchrotron Radiat*., 2013, **20**, 923-928.
(29) S. Matsuoka, S. Sugiyama, D. Matsuoka, M. Hirose, S. Lethu, H. Ano, T. Hara, O. Ichihara, S. R. Kimura, S. Murakami, H. Ishida, E. Mizohata, T. Inoue, M. Murata, *Angew. Chem. Int. Ed.,* 2015, **54**, 1508–1511.
(30) G. F. Crouse, A. Frischauf, H. Lehrach in "Methods in Enzymology", Vol. 101, pp. 78. Eds: R. Wu, Academic Press, New York, 1983.
(31) H. N. Madhavan, J. Malathi, R. P. Joseph, Y. Mori, S. J. K. Abraham,H. Yoshioka, *Curr. Sci.* 2004, **87**, 1275−1277..
(32) H. Yoshioka, M. Mikami, Y. Mori, E. Ttsuchida, *J. Macromol. Sci, Part A*., 1994, **31**, 113–120.
(33) H. Yoshioka, M. Mikami, Y. Mori, E. Tsuchida, *J. Macromol. Sci, Part A*., 1994, **31**, 121–125.
(34) H. Yoshioka, Y. Mori, J. A. Cushman, *Polym Adv Tech.*, 1994, **5**, 122–127.
(35) N. Parveen, A. A. Khan, S. Baskar, M. A. Habeeb, R. Babu, S. Abraham, H. Yoshioka, H. C. Mohammed, *Hepatitis Monthly*, 2008, **8**, 275–280.
(36) Otwinowski, Z.; Minor, W.; *Methods Enzymol* **1997**, 276, 307–326.
(37) L. Pugliese, A. Coda, M. Malcovati, M. Bolognesi, *J. Mol. Biol.*, 1993, **231**, 698−710.
(38) P. Emsley, and K. Cowtan, *Acta Crystallogr.,* 2004, **D60**, 2126–2132.
(39) A. T. Brünger, P. D. Adams, G. M. Clore, W. L. DeLano, P. Gros, R. W. Grosse-Kunstleve, J.-S. Jiang, J. Kuszewski, M. Nilges, N. S. Pannu, R. J. Read, L. M. Rice, T. Simonson, G. L. Warren, *Acta Crystallogr.,*1998, **D54**, 905–921.
(40) R. A. Laskowski, M. W. MacArthur, D. S. Moss, J. M. Thornton, *J. Appl. Cryst.*, 1993, **26**, 283–291.
(41) C. Sauter, B. Lorber, R. Giege, *Proteins,* 2002, **48**, 146–150.
(42) J. A.Gavira, J. M. Garcia-Ruiz, *Acta Crystallogr.,* 2002, **D58**, 1653–1656.

Figure legends

Figure 1

Photographs of seeding experiments with hydrogel-grown seed crystals. (a) Schematic diagram of the protocol for transporting seed crystals using a combination of high-strength hydrogel and macroseeding methods. (b) Photographs of agarose-grown FABP3 seed crystal before seeding, just after seeding, and after 1 to 14 days. (c) Photographs of agarose-grown LZM seed crystal before seeding (left) and after 58 days (right). (d) Photographs of TGP-grown LZM seed crystal before seeding (left) and after 60 days (right). (c, d) The dotted circles indicate seed crystals. The hydrogel-grown crystals can be seen at the center of the large crystals.

Figure 2

Photographs of spontaneous nucleation during macroseeding experiments. (a) Agarose-grown FABP3 seed crystals grown at protein concentrations of 6mg/ml just after seeding (left) and after 7 days (right). (b) Agarose-grown FABP3 seed crystals grown at protein concentrations of 9mg/ml just after seeding (left) and after 7 days (right). (c) Agarose-grown LZM seed crystals grown at protein concentrations of 20mg/ml after 7 days. (d) TGP-grown LZM seed crystals grown at protein concentrations of 20 mg/ml after 7 days.

Figure 3

XRD patterns of hydrogel-grown and seed-grown crystals. (a) Agarose-grown FABP3 crystal. (b) As-grown FABP3 crystal containing agarose-grown seed crystal. (c) Agarose-grown LZM crystal. (d) Seed-grown LZM crystal containing agarose-grown seed crystal. (e) TGP-grown LZM crystal. (f) TGP-grown LZM crystal containing TGP-grown seed crystal.

Figure 4

Electron density maps contoured at 2.0σ with ($2|F_o|-|F_c|$) amplitudes. These maps are calculated using the diffraction data from hydrogel-grown and seed-grown crystals. (a) Agarose-grown seed and seed-grown FABP3 crystals. The map resolution of agarose-grown FABP3 crystals is 1.50Å, and that of seed-grown FABP3 crystals is 1.60Å. (b) Agarose-grown seed and seed-grown LZM crystals. The map resolution of agarose-grown LZM crystals is 1.50Å, and that of seed-grown LZM crystals is 1.55Å. (c) TGP-grown seed and seed-grown LZM crystals. The map resolutions of TGP-grown and seed-grown LZM crystals are 1.50Å.

Table 1. Crystallization and seeding conditions

Proteins (source)	FABP3 (human)	LZM (chicken egg-white)
Crystallization conditions		
Hydrogel conc. (w/v)	1.5% agarose	1.5% agarose, or 5.0% TGP
Protein conc. (mg/ml)	20	20
Precipitant agent (w/v)	20% PEG400	3.0% NaCl
Buffer	0.1M Tris-HCl	0.1M Na acetate
pH	8.5	4.5
Seeding conditions		
Protein conc. (mg/ml)	3	10
Precipitant agent (w/v)	20% PEG400	3.0% NaCl
Buffer	0.1M Hepes-NaOH	0.1M Na acetate
pH	8.5	4.5

Table 2 X-ray diffraction data statistics

Proteins	FABP3	FABP3	Lysozyme	Lysozyme	Lysozyme	Lysozyme	Lysozyme	Lysozyme
Crystals grown in	Agarose	Agarose	Agarose	Agarose	Agarose	TGP	TGP	TGP
Crystals	Seed	Seed-grown	Seed	Seed-grown-1	Seed-grown-2	Seed	Seed-grown-1	Seed-grown-2
Source	In-house	In-house	In-house	SPring-8	SPring-8	SPring-8	SPring-8	SPring-8
Detector	R-axis V	R-axis V	R-axis V	MX225HE	MX225HE	MX225HE	MX225HE	MX225HE
Wavelength (Å)	1.54	1.54	1.54	0.90	0.90	0.90	0.90	0.90
Space group	$P2_12_12_1$	$P2_12_12_1$	$P4_32_12$	$P4_32_12$	$P4_32_12$	$P4_32_12$	$P4_32_12$	$P4_32_12$
Unit-cell parameters (Å)								
a	54.5	54.6	78.4	78.2	77.6	78.1	78.0	78.1
b	70.0	70.2	78.4	78.2	77.6	78.1	78.0	78.1
c	33.9	33.9	36.9	37.0	37.2	37.2	37.4	37.3
Resolution (Å)	50 – 1.50	50 – 1.50	50 – 1.50	50 – 1.60	50 – 1.50	50 – 1.50	50 – 1.55	50 – 1.50
(High-resolution shell)	(1.53 – 1.50)	(1.53 – 1.50)	(1.53 – 1.50)	(1.63 – 1.60)	(1.53 – 1.50)	(1.53 – 1.50)	(1.58 – 1.55)	(1.53 – 1.50)
No. of reflections	144,478	133,111	266,835	189,495	234,705	102,166	215,964	241,359
Oscillation angle (°)	0.25	0.25	1.00	1.00	1.00	1.00	1.00	1.00
Total rotation angle (°)	180	180	200	180	180	90	180	180
No. of unique reflections	21,419	21,448	19,055	15,804	18,810	17,875	17,249	19,109
Redundancy	6.7 (5.3)	6.2 (4.0)	14.0 (7.4)	12.0 (10.5)	12.5 (11.0)	5.7 (2.0)	12.5 (10.6)	12.6 (10.5)
Mean $I/\sigma(I)$	42.4 (23.9)	42.0 (17.2)	32.1 (15.0)	7.0 (2.7)	7.4 (2.3)	18.9 (8.4)	9.7 (4.8)	9.0 (3.1)
Completeness (%)	99.4 (89.6)	99.0 (93.0)	99.8 (98.9)	99.9 (99.9)	100 (99.9)	93.9 (83.1)	99.2 (98.1)	99.2 (99.8)
R_{merge} (%)[a]	2.6 (7.8)	3.8 (9.3)	5.0 (15.3)	9.3 (57.8)	8.4 (58.1)	6.9 (10.8)	6.7 (57.6)	5.7 (50.9)
R_{pim} (%)	1.1 (3.6)	1.6 (5.0)	1.4 (5.9)	2.7 (18.3)	2.4 (18.0)	2.9 (8.7)	1.9 (18.2)	1.6 (16.0)
$CC_{1/2}$ in high-resolution	0.99	0.98	0.98	0.83	0.85	0.96	0.93	0.86
Mosaicity (°)	0.52	0.51	0.57	0.49	0.42	0.34	0.36	0.33
Refinement								
Resolution range (Å)	43.04 – 1.50	43.04 – 1.50	55.51 – 1.50	55.51 – 1.60	54.91 – 1.50	55.23 – 1.50	55.19 – 1.55	55.26 – 1.50
No. of reflections	20,275	20,329	18,032	14,983	17,811	16,928	16,350	18,102
R_{cryst}[b] / R_{free}[c]	0.15 / 0.18	0.15 / 0.18	0.16 / 0.17	0.17 / 0.21	0.18 / 0.22	0.16 / 0.19	0.17 / 0.20	0.17 / 0.19
No. of water molecules	174	178	177	177	172	137	139	145
RMSD bond length (Å)	0.024	0.023	0.019	0.019	0.019	0.021	0.019	0.022
RMSD bond angle (°)	2.2	2.2	1.9	1.8	1.8	2.0	1.9	2.0

a. $R_{merge} = \sum_{hkl}\sum_i |I_i(hkl) - \langle I(hkl)\rangle| / \sum_{hkl}\sum_i I_i(hkl)$, where $I_i(hkl)$ is the *i*th observed intensity of reflection *hkl* and $\langle I(hkl)\rangle$ is the average intensity over symmetry-equivalent measurements. Values in parentheses are for the highest resolution shell.

b. $R_{cryst} = \Sigma\,||F_o| - |F_c||/\,\Sigma\,|F_o|$ calculated from 95% of the data, which were used during refinement.

c. $R_{free} = \Sigma\,||F_o| - |F_c||/\,\Sigma\,|F_o|$ calculated from 5% of the data, which were used during refinement.

Figure 1.

(a)

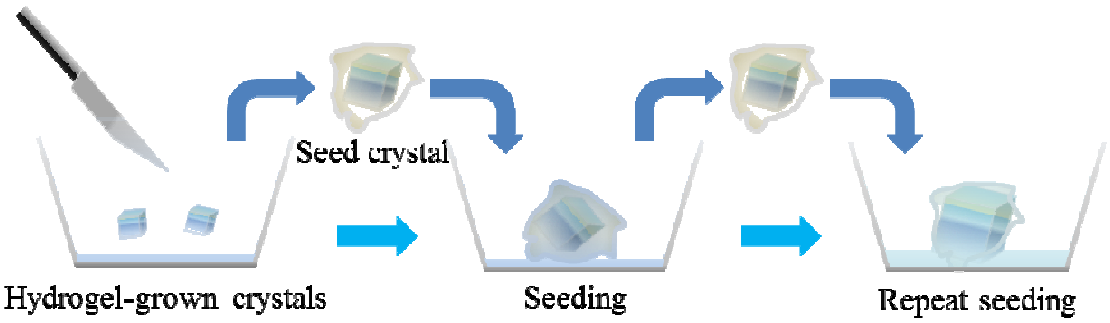
Seed crystal
Hydrogel-grown crystals
Seeding
Repeat seeding

(b)

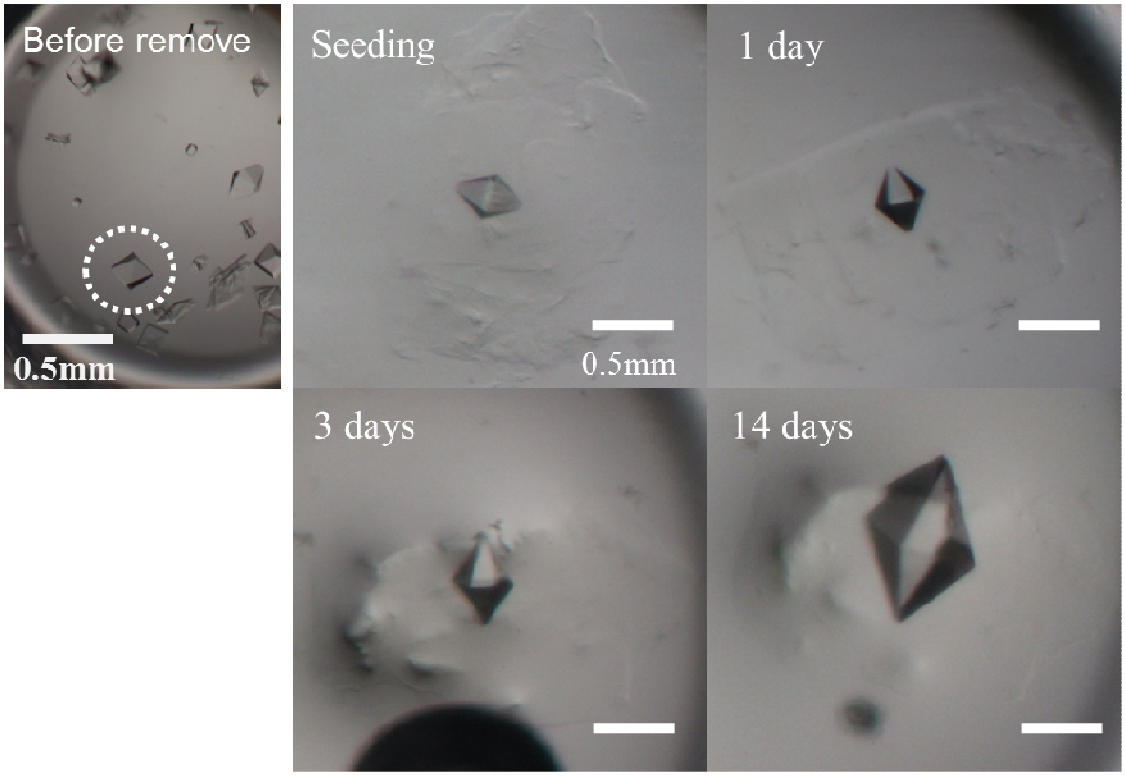
Before remove
0.5mm
Seeding
0.5mm
1 day
3 days
14 days

Figure 1.

(c)

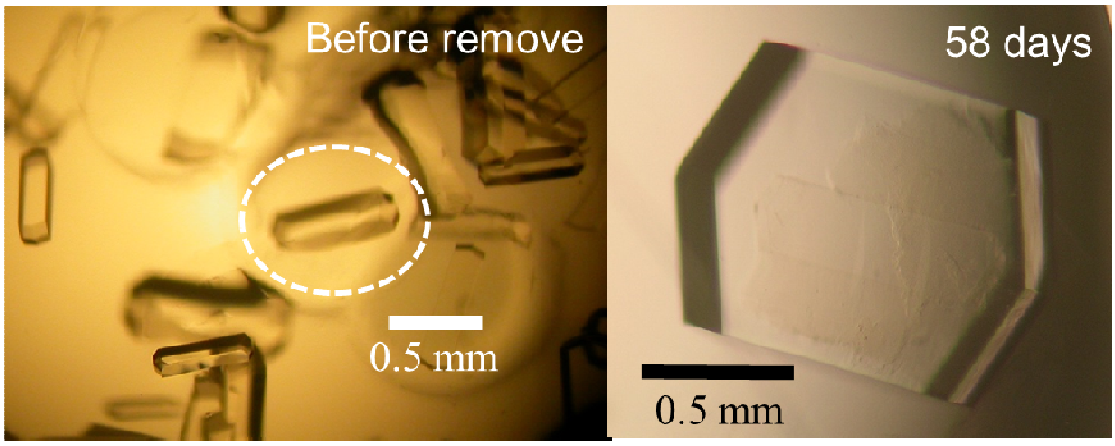
Before remove
0.5 mm
58 days
0.5 mm

(d)

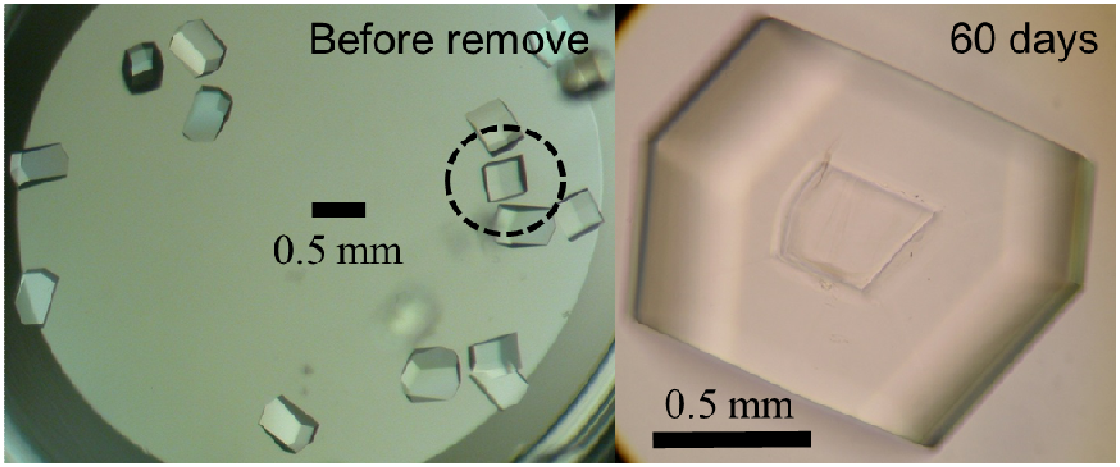
Before remove
0.5 mm
60 days
0.5 mm

Figure 2.

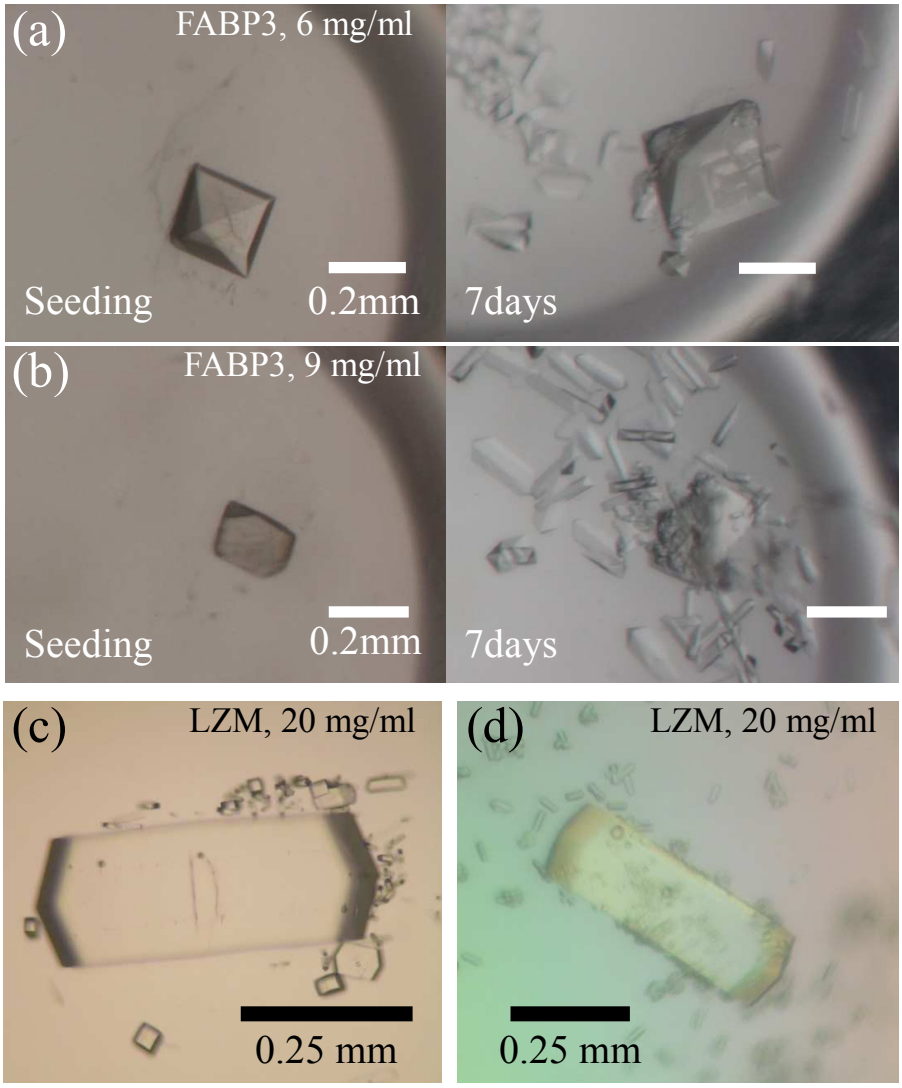
(a)
FABP3, 6 mg/ml
Seeding
0.2mm
7days
(b)
FABP3, 9 mg/ml
Seeding
0.2mm
7days
(c)
LZM, 20 mg/ml
0.25 mm
(d)
LZM, 20 mg/ml
0.25 mm

Figure 3.

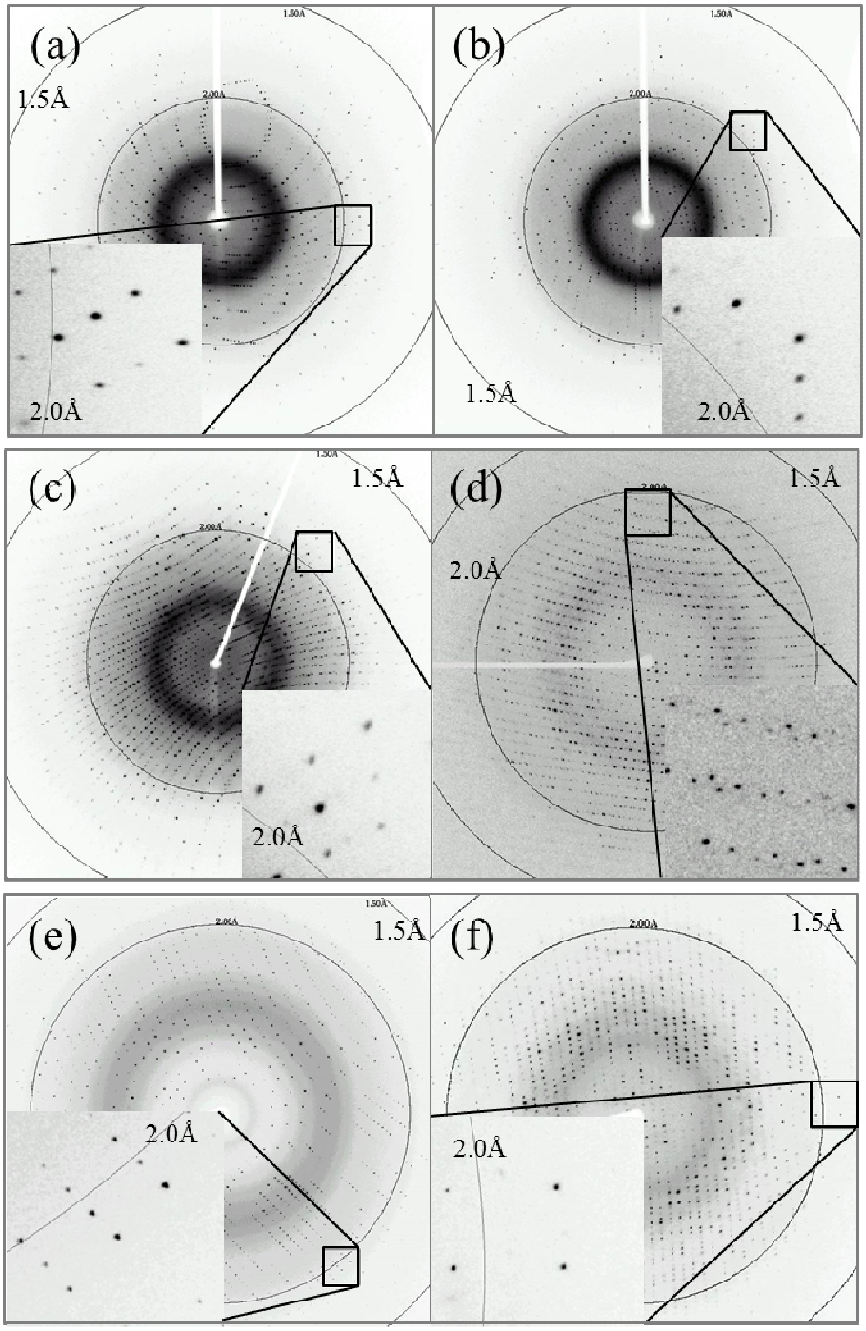

Figure 4.

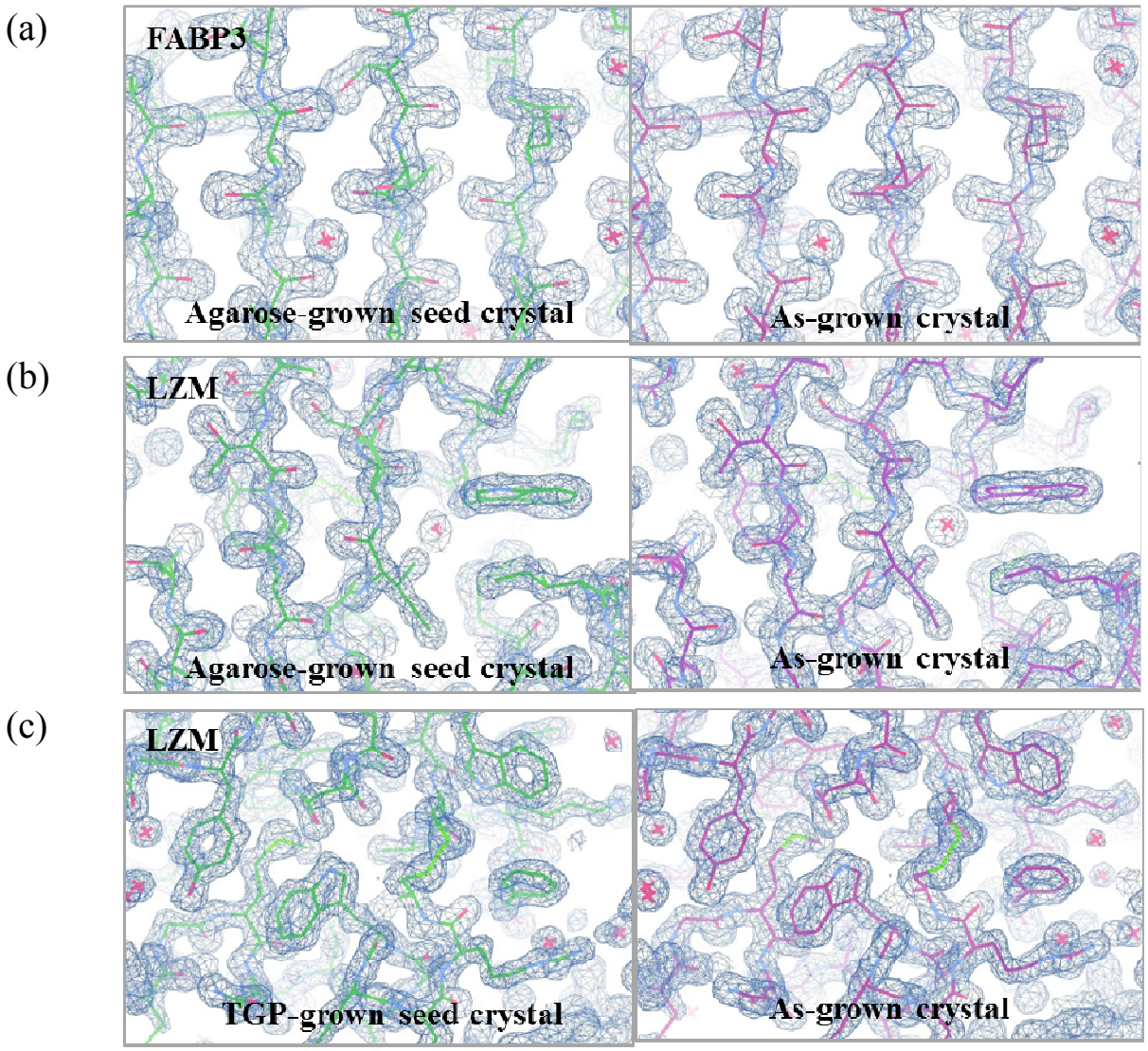
(a)
FABP3
Agarose-grown seed crystal
As-grown crystal
(b)
LZM
Agarose-grown seed crystal
As-grown crystal
(c)
LZM
TGP-grown seed crystal
As-grown crystal